
aLIGO bow-tie Pre-Modecleaner document

LIGO-T-0900616-v3

Jan Hendrik Pöld (jan.poeld@aei.mpg.de)

This document was prepared in the design phase of the new Pre-Modecleaner (PMC) for Advanced LIGO. The current version is updated after building all aLIGO PMCs. A list of assumptions and calculations including the values for the simulation of the PMC can be found. Furthermore a prototype PMC was built and tested. The comparison with the design parameters shows that the properties of this prototype are in accordance with the parameters and tolerances that were calculated.

Contents

1	Introduction	1
1.1	Requirements	1
2	Design	1
2.1	Spacer	1
2.2	Tank	1
2.3	Components	2
2.4	Gluing	2
2.5	Long range actuation	2
2.6	Internal power buildup	3
2.7	Power noise	3
3	Simulations	3
3.1	Calculation of design parameters	4
3.2	Accuracy simulation	4
3.3	Monte-Carlo simulation	4
4	Performance	4
4.1	Properties and tolerances	5

4.2	Polarization	5
4.3	Pointing noise suppression	6
4.4	Suppression of rf power noise	6
4.5	Heater performance	6

Max-Planck-Institute for Gravitational Physics
Albert-Einstein-Institute
Callinstrasse 38
30167 Hannover

1 Introduction

The development of a Pre-Modecleaner (PMC) responsible for spatial beam filtering and suppression of power noise at radio frequencies, is presented in this document. A detailed design study (Sec. 2) and simulations (Sec. 3) in order to determine reasonable parameters and tolerances are shown. Test with a PMC prototype were performed and the accordance with the predicted design parameters is discussed in Section 4.

1.1 Requirements

The relevant requirements that have to be fulfilled by the Advanced LIGO PMC can be found in the design requirement document (T-050036).

2 Design

Generally the PMC consists of a spacer with mirrors glued to it that is housed inside a tank (aLIGO PSL PMC mechanical drawings). The resonator design is a bow-tie shape, because the round trip length only scales appreciably with the extension in one dimension. A small extension in the other direction leads to a small angle of incidence on the mirrors. In this configuration there are four ports available. Two of them are used for input and output coupling for the main beam. The remaining two can be used as monitor ports with the advantage that the light exiting those is filtered by the PMC.

This section deals with the design of the new aLIGO PMC and aspects that have to be considered in the design phase.

2.1 Spacer

The spacer is a 507 mm long and 160 mm wide rigid aluminum block (aLIGO PSL PMC mechanical drawings) which has a weight of 16 kg. However, it is beveled at both sides to provide a surface where the mirrors can be glued directly. Although the PMC is symmetric, the spacer is not, because additional space for the PZT has to be considered. There are special requirements for the parallelism of the fronts in order to avoid tilts of the mirrors. The accuracy of the 12 mm drills is also important, such that the beam would not clip inside the PMC.

2.2 Tank

Some contamination was found on the mirrors of the PMC which is currently in initial LIGO after long term operation with optical load. Therefore the Advanced LIGO PMC will be housed in an aluminum tank (aLIGO PSL PMC mechanical drawings). Additionally this tank acts as an acoustic shielding, thermal enclosure and as dust protection. Viton pads are lying between the tank and the spacer so that there is a reduced heat transfer and some damping of mechanical vibrations and the spacer is clamped down to the bottom of the tank. The tank has a length of 590 mm and a width of 250 mm. Four 0.5° wedged windows provide a possibility for the beam

to enter and leave the tank. They are glued to an aluminum adapter and then screwed to the tank. The windows are angled by 15 deg with respect to the cavity eigenmode.

2.3 Components

For an optimal performance at high power optical components need to have very high quality. In particular super polished fused silica substrates with 1 inch diameter are used to achieve a low amount of stray light. The thermal heat up has to be very small, as this would cause a change of curvature due to thermal effects. Especially HR and AR coatings have to have nearly ideal properties. The substrates that are being used for the incoupler and outcoupler were coated within the same coating run in order to have only small differences of their properties.

The PZT used for Pound-Drever-Hall locking is able to change the round trip length by $2.5 \mu\text{m}$ which corresponds 2.5 FSR with a high voltage range from 0 V to 400 V.

2.4 Gluing

The assembly of the PMC is done in the clean room to avoid any dust particles from entering the cavity. Vacuum compatible glue (Master Bond EP 30-2) is used to fix the mirrors on the surface of the spacer. One of the curved mirrors is glued to a PZT which is glued to the spacer. The other three mirrors are directly glued to the spacer. Removable gluing adapters are used to hold the mirrors in the right position until the glue is fixed. Before gluing the last mirror to the spacer a laser beam is injected so that the mirror can be placed to the correct position. The tolerances that are assumed in the gluing process are summarized in table 1. A simulation was done which showed that these tolerances are acceptable such that a closed beam path is still guaranteed.

2.5 Long range actuation

The long range actuation of the PMC is achieved by heating the spacer. Knowing the thermal expansion coefficient $\alpha = 23.1 \mu\text{m} \cdot (\text{K})^{-1}$ the behavior of the PMC is calculated, so that

$$\frac{L \cdot \alpha}{\lambda} = 43 \frac{\text{FSR}}{\text{K}}. \quad (1)$$

Hence a PMC resonance frequency is shifted by 43 FSR when the temperature is raised by 1 K. The goal is to have a dynamic range of $\Delta T = 5 \text{ K}$ and therefore two thermal Kapton pads are glued to the spacer, each of them with a resistance of 52Ω . For monitoring of the temperature an AD 590 integrated circuit temperature transducer is mounted on top of the spacer.

Translation of curved mirrors	$\pm 0.001 \text{ m}$
Tilt of curved mirrors	$\pm 0.1 \text{ deg}$
Tilt of flat mirrors	$\pm 0.1 \text{ deg}$
Tolerances of spacer parameters	$\pm 0.001 \text{ m}$

Table 1: Acceptable tolerances for the gluing and production process of the PMC.

The supply voltage that is provided by the electronics is 24 V which leads to a maximum electrical power of 20 W which is converted into heat by the thermal pad. Adjustments of the current through the heat pads can be done via software of the computer control in order to keep the PMC at a temperature such that the PZT stays in the middle of the range.

2.6 Internal power buildup

There is a power buildup inside the cavity depending on the transmission of the four mirrors. Thus considerations of the thermal loading have to be made. No thermal lens effects were observed with the old triangular PMC which was tested in long term experiments. This cavity has a Finesse of 383 and was illuminated with a 35 W front end laser and a peak intensity of

$$I_{0,\text{peak}}(\omega_0 = 372 \mu\text{m}) = 1,963 \cdot 10^6 \frac{\text{W}}{\text{cm}^2}. \quad (2)$$

The optical load on the mirrors of the new design should not exceed the old value calculated in the latter equation.

2.7 Power noise

The dominating source for power noise at radio frequencies is the one of the NPRO. The shot noise for a photo current of 100 mA is

$$N_S = \sqrt{\frac{2 \cdot q}{I}} = 1.79 \cdot 10^{-9} \frac{1}{\sqrt{\text{Hz}}} \quad (3)$$

and since shot noise and technical noise are independent, they add quadratically such that the requirement can be written as

$$1,122 \cdot N_S \geq \sqrt{N_T^2 + N_S^2} \quad (4)$$

$$N_T \leq 9.11 \cdot 10^{-10} \frac{1}{\sqrt{\text{Hz}}}.$$

Upstream of the PMC the technical noise N_T is at 9 MHz according to a model of the NPRO power noise¹ 21.05 dB above the noise level required downstream of the PMC. Hence the transfer function of the PMC has to be below -21.05 dB at 9 MHz which corresponds to a maximum PMC bandwidth of 800.69 kHz.

3 Simulations

Three simulations were done in order to define the final design parameters. A calculation of the PMC properties (Sec. 3.1, an estimation of the accuracy of the mechanical design (Sec. 3.2) and a Monte-Carlo simulation that simulates several PMCs in between the given tolerances.

¹P. Kwee, and B. Willke, Automatic laser beam characterization of monolithic Nd:YAG nonplanar ring lasers. Applied Optics. 2008.

3.1 Calculation of design parameters

A program was developed which simulates a PMC with given start values. At the end of the routine a test to check whether all design requirements are fulfilled is done. The final set of parameters and their estimated tolerances is listed in table 2.

The tolerances for the transmission of the mirrors were given by the supplier, all other tolerances are estimated. Considering the final start values, the simulated PMC properties can be calculated as shown in table 3.

3.2 Accuracy simulation

The assumptions for the accuracy of the spacer drillings and the tolerances of the aluminum spacer are based on the output of a simulation that does a ray tracing to look if there is a close beam path inside the resonator. The tilts of all mirrors, a transverse shift of the curved mirrors and an upper boundary for the deviation from the initial path are the values that can be varied in the program (Tab. 1). The routine simulates the PMC with all possible combinations of the tolerance value to check if the parameters still obey the boundary conditions.

3.3 Monte-Carlo simulation

To check the accordance with the requirements with respect to the given tolerances a Monte-Carlo simulation was performed. In almost all of the one million cycles the simulated PMC was able to meet the design requirements. The resulting tolerances for the properties of the PMC are illustrated in table 4.

4 Performance

In this section a comparison of the predicted design properties with the prototype version of the PMC is presented.

Transmission of flat mirrors	0.0248 ± 0.001
Absorption of flat mirrors	$5e-006 \pm 0.0001$
Transmission of curved mirrors	$6.8e-005 \pm 1e-005$
Absorption of curved mirrors	$5e-006 \pm 0.0001$
Radius of curvature	$3 \text{ m} \pm 0.15 \text{ m}$
Spacer long side	$0.5 \text{ m} \pm 0.002 \text{ m}$
Spacer short side	$0.1 \text{ m} \pm 0.002 \text{ m}$
Internal aperture radius at waist	$0.004 \pm 0.0001 \text{ m}$

Table 2: PMC design parameters and their estimated tolerances. The values for the absorption is an assumption for the Monte-Carlo simulation and is varied from 0 ppm to 105 ppm.

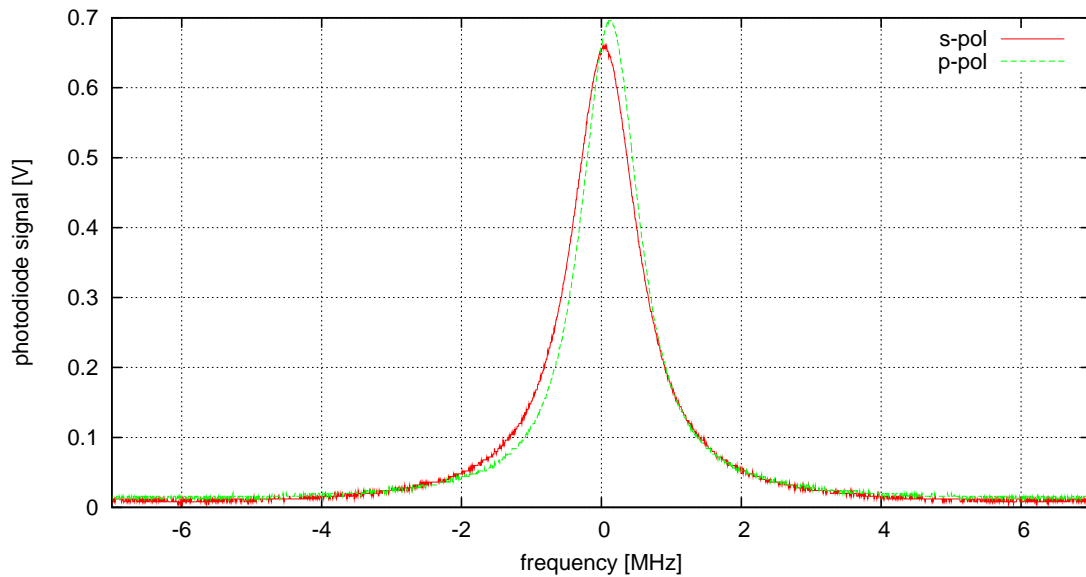


Figure 1: Polarization dependence of the PMC prototype

4.1 Properties and tolerances

The information listed in table 5 show a comparison of the experimentally measurable parameters of the prototype PMC² with the theoretical calculated ones. The measured values for the impedance matching and the throughput can just be considered as upper boundaries, due to the experimental setup where they were measured. All other parameters are in the range of the estimated tolerances.

4.2 Polarization

According to the Fresnel equations, reflected beams with a polarization perpendicular to the plane of the resonator obtain an extra phase shift by a factor π . Since the beam is reflected at four surfaces the additional phase shift should not affect the resonance condition. As shown in Figure 1 this could be verified in a setup where a beam containing a mixed polarization is injected into the PMC. The transmitted beam is divided by a polarizing beam splitter and both beams are detected on a PD. The slight difference in the resonance frequency could be due to a different depth of penetration into the mirror coatings of s- and p-polarized beams. Thus the resonator length is changing by a small amount which leads to a shift of the resonance peaks. In contrast to the three mirror cavity, a resonator with a bow-tie configuration provides no polarization filtering.

²Transmission of curved mirrors of the PMC prototype: 3 ppm. According to the simulations this should not affect the other properties, except the monitor output powers, significantly.

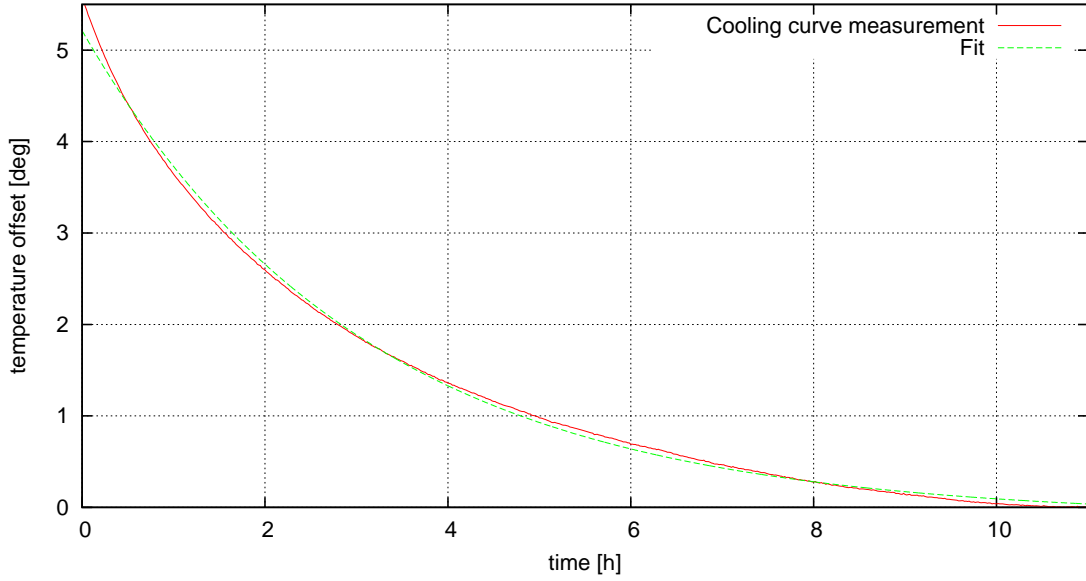


Figure 2: Cooling curve of the PMC prototype. The heater range is 5.2 K and the time constant is 3.05 hours.

4.3 Pointing noise suppression

In the Eigenbasis of the PMC pointing, described by $|\epsilon|$ can be interpreted in first approximation as an excitation of first order TEM modes. Since these modes are not resonant the suppression depends on the Gouy-phase and the Finesse such that the PMC prototype should attenuate the pointing by

$$S = \sqrt{\frac{1}{1 + \frac{(2\mathcal{F})^2}{\pi^2} \cdot \sin^2\left(\frac{\zeta}{2}\right)}} = 0.0164. \quad (5)$$

4.4 Suppression of rf power noise

The PMC provides a suppression of power noise at radio frequencies. Since the PMC has a low pass behavior the attenuation factor depends on the bandwidth of the PMC that corresponds half of the FWHM listed in table 1.

4.5 Heater performance

Experimental data were acquired to see whether it is possible with the given heat power to have the expected dynamic range. Figure 2 shows the cool down of the spacer after it reached its thermal equilibrium with full heat power. The behavior could be described by Newtons law of cooling

$$T(t) = T_{\text{env}} + (T(0) - T_{\text{env}}) \cdot e^{-\frac{t}{\tau}} \quad (6)$$

where T_{env} is the temperature of the environment, $T(0)$ is the temperature at $t=0$ and τ is the time constant of the system, which describes the thermal contact to the environment.

A dynamic range of 5.21 K matches the goal. Further experiments show that the PMC stays in lock when the room temperature is varying by more than 2 K. The characteristic time constant is measured to be 3.05 hours.

Finesse	124.708
Round-trip length	2.02 m
Intra-Cavity Power (@ 200W input)	7865.65 W
Thermal actuator coefficient	43.851 FSR/K
Free spectral range	148.529 MHz
FWHM	1.19 MHz
Relative powers at the output ports (output, monitor)	0.994, 0.00266
Impedance matching	1
Throughput	0.994
Average power built-up	39.33
Incidence angle	0.0987 rad
Round trip Gouy phases in x- and y-direction	1.754, 1.744 rad
Pointing suppression in x- and y-direction	0.0163, 0.01644
Peak relative intensities at mirror surfaces	7950 1/cm ² , 4800 1/cm ²
Quality of eigenmode due to ellipticity	1
Ellipticity	0.995
Averaged waist of input/output beam	547.688 μm
Averaged waist between curved mirrors	711.782 μm
Highest possible mode order	53
Lowest mode order with less than 0.1 suppression	18

Table 3: PMC properties that meet the Advanced LIGO requirements.

Finesse	124.536 ± 5.091
Round-trip length	$2.02 \text{ m} \pm 0.008 \text{ m}$
Intra-Cavity Power (@ 200W input)	$7831.44 \text{ W} \pm 323.501 \text{ W}$
Thermal actuator coefficient	$43.85 \text{ FSR/K} \pm 0.17 \text{ FSR/K}$
Free spectral range	$148.532 \text{ MHz} \pm 0.585 \text{ MHz}$
FWHM	$1.195 \text{ MHz} \pm 0.0488 \text{ MHz}$
Impedance matching	$1 \pm 5.5\text{e-}005$
Throughput	0.988 ± 0.007
Average power built-up	39.16 ± 1.62
Incidence angle	$0.0987 \text{ rad} \pm 0.002 \text{ rad}$
Round trip Gouy phases in x- and y-direction	$1.757 \text{ rad} \pm 0.052 \text{ rad},$ $1.747 \text{ rad} \pm 0.052 \text{ rad}$
Pointing suppression in x- and y-direction	$0.0165 \pm 0.0008,$ 0.0165 ± 0.0008
Peak relative intensities at mirror surfaces	$7936 \text{ 1/cm}^2 \pm 468 \text{ 1/cm}^2,$ $4780 \text{ 1/cm}^2 \pm 202 \text{ 1/cm}^2$
Quality of Eigenmode due to ellipticity	$1 \pm 1.26\text{e-}005$
Ellipticity	0.995 ± 0.0003
Averaged waist of input/output beam	$547.094 \mu\text{m} \pm 7.48856 \mu\text{m}$
Averaged waist between curved mirrors	$711.974 \mu\text{m} \pm 1.963\text{e-}006 \mu\text{m}$
Highest possible mode order	53.08 ± 3.82
Lowest mode order with less than 0.1 suppression	19.79 ± 9.45

Table 4: Monte-Carlo simulation of the PMC with 1000000 cycles.

Properties	Monte-Carlo	PMC prototype
Finesse	124.536 ± 5.091	120.44 ± 0.6
Thermal actuator coefficient	$43.85 \text{ FSR/K} \pm 0.17 \text{ FSR/K}$	
Free spectral range	$148.532 \text{ MHz} \pm 0.585 \text{ MHz}$	$148.32 \text{ MHz} \pm 0.742 \text{ MHz}$
FWHM	$1.195 \text{ MHz} \pm 0.0488 \text{ MHz}$	$1.19 \text{ MHz} \pm 0.06 \text{ MHz}$
Impedance matching	$1 \pm 5.5e-005$	0.9925 ± 0.005
Throughput	0.988 ± 0.007	0.9815 ± 0.005
Round trip Gouy phases in x- and y-direction	$1.757 \text{ rad} \pm 0.052 \text{ rad},$ $1.747 \text{ rad} \pm 0.052 \text{ rad}$	$1.718 \text{ rad} \pm 0.003 \text{ rad},$ $1.714 \text{ rad} \pm 0.003 \text{ rad}$

Table 5: Theoretically calculated and measured PMC properties and tolerances.